

Explanations of the Tentative New Physics Anomalies and Dark Matter in the Simple Extension of the Standard Model (SESM)

Tianjun Li,^{1,2,*} Junle Pei,^{1,2,†} Xiangwei Yin,^{1,2,‡} and Bin Zhu^{3,§}

¹*CAS Key Laboratory of Theoretical Physics, Institute of Theoretical Physics,
Chinese Academy of Sciences, Beijing 100190, China*

²*School of Physical Sciences, University of Chinese Academy of Sciences,
No. 19A Yuquan Road, Beijing 100049, China*

³*Department of Physics, Yantai University, Yantai 264005, China*

Abstract

We revisit the Simple Extension of the Standard Model (SESM) which can account for various tentative new physics anomalies and dark matter (DM). We consider a complete scalar potential which is needed to address the W boson anomaly. Interestingly, the SESM can simultaneously explain the B physics anomaly, muon anomalous magnetic moment, W mass anomaly, and dark matter, etc. Also, we study the unitarity constraint in this model. We perform the systematic study, and find the viable parameter spaces which can explain these anomalies and evade all the current experimental constraints. To be complete, we briefly comment on the neutrino masses and mixings, baryon asymmetry, and inflation.

* tli@mail.itp.ac.cn

† peijunle@mail.itp.ac.cn

‡ yinxiangwei@mail.itp.ac.cn

§ zhubin@mail.nankai.edu.cn

CONTENTS

I. Introduction	3
II. The Simple Extension of the Standard Model	4
III. The Unitarity Constraint	6
A. The unitarity constraint of λ_2^Q	7
1. $J = 0$ partial wave	7
B. A brief summary of the unitarity constraints in Yukawa sector	8
IV. The Tentative New Physics Anomalies and Dark Matter	9
A. R_K and B_s mixing	9
B. Muon $g-2$	10
C. Dark matter phenomenology	10
V. W Boson Mass	14
VI. Conclusion	16
Acknowledgments	17
A. The Unitarity Constraint on λ_2^Q	17
1. The Unitarity Constraint on λ_2^Q	17
a. $J = 0$ Partial Wave	17
b. $J = \frac{1}{2}$ Partial Wave	18
2. The Unitarity Constraint on λ_3^Q	18
3. The Unitarity Constraint on λ_2^L	19
a. $J = 0$ Partial Wave	19
b. $J = \frac{1}{2}$ Partial Wave	19
4. The Unitarity Constraint on λ_2^E	20
a. $J = 0$ Partial Wave	20
b. $J = \frac{1}{2}$ Partial Wave	21
References	21

I. INTRODUCTION

After the discovery of Higgs boson at the LHC in 2012 [1, 2], the Standard Model (SM) has been confirmed to be a correct effective theory at the low energy scale. However, we do have a few evidences of new physics Beyond the SM (BSM), for instance, dark energy, dark matter (DM), neutrino masses and mixings, baryon asymmetry, and inflation, etc [3]. Also, there exist some fine-tuning problems in the SM, for example, gauge hierarch problem, and strong CP problem, etc. Thus, the SM is not complete, and we need to explore the new physics.

In recent years, the LHCb Collaboration has declared the results in rare decays of B mesons. The persistent discrepancies between the Standard Model and the experimental measurements imply that there might be new physics. Such B physics anomalies can be observed in the angular distribution of $B \rightarrow K\mu^+\mu^-$ and Lepton Flavor Universality (LFU) ratios $R_K = BR(B \rightarrow \mu\mu)/BR(B \rightarrow ee)$ [4–8]. Also, there exists a 4.2σ discrepancy for the muon anomalous magnetic moment (muon $g - 2$) $a_\mu = (g_\mu - 2)/2$ between the experimental results and theoretical predictions [9]. Although the hadronic contribution might induce the discrepancy, muon $g - 2$ is still a promising hint for new physics beyond the SM [12–14], and has been studied extensively [15–19]. Recently, the CDF Collaboration announced a state-of-the-art measurement of the W boson mass, which shows 7σ deviation from the prediction of the SM [20]. For recent studies, see Refs. [21–60]. Moreover, the DM is a crucial problem in both particle physics and astronomy, and the observations from astrophysics and cosmology provide the overwhelming evidence. The Weakly Interacting Massive Particle (WIMP) provide an excellent DM candidate to account for the relic density observed by the experiment of Cosmic Microwave Background (CMB). This is the so called “WIMP miracle”.

To address the above anomalies and dark matter, we revisit the Simple Extension of the Standard Model (SESM) [61]. We consider a complete scalar potential which is needed to account for the W boson anomaly. Interestingly, the SESM can simultaneously explain the B physics anomaly, muon anomalous magnetic moment, W boson mass anomaly, and dark matter, etc. Also, we study the unitarity constraint in this model. We perform the systematic study, and find the viable parameter spaces which can explain these anomalies and evade all the current experimental constraints. To be complete, similar to the New

Minimal SM (NMSM) [3], we can introduce two right-handed neutrinos to explain the neutrino masses and mixing as well as baryon asymmetry, and introduce a real scalar to address inflation. Because of the strong constraint on the tensor-to-scalar ratio, we need to choose the proper inflaton potential, for example, the inflaton potentials in Section 2 of Ref. [62]. The XENON1T excess [63] will be studied elsewhere as well.

This paper is organized as follows. In Section II, we briefly review the SESM and present the complete scalar potential. In Section III, the constraints of unitarity on the parameters in the Yukawa sector are studied. In Section IV, we explain the above anomalies and dark matter. In Section V, the W boson mass anomaly is investigated. We conclude in Section VI.

II. THE SIMPLE EXTENSION OF THE STANDARD MODEL

Following Ref. [61] we introduce a complex singlet scalar Φ_S , a doublet scalar Φ_D , and two vectorlike pairs of Weyl fermions (that combine into two Dirac fermions) with the same quantum numbers as the SM quark and lepton doublets Q' and L' . Under a discrete Z_2 symmetry, these extra fields are all odd while the SM fields are even. The quantum numbers of extotic fields under SM gauge group are

Field	spin	$SU(3)_c$	$SU(2)_L$	$U(1)_Y$
Q'	1/2	3	2	1/6
L'	1/2	1	2	-1/2
Φ_S	0	1	1	0
Φ_D	0	1	2	-1/2

(1)

The new vectorlike fermions and scalars can be written as

$$Q' = \begin{pmatrix} U' \\ D' \end{pmatrix}, \quad L' = \begin{pmatrix} L'^0 \\ L'^- \end{pmatrix}, \quad \Phi_S \equiv S_s^0, \quad \Phi_D = \begin{pmatrix} S_d^0 \\ S^- \end{pmatrix}. \quad (2)$$

The Lagrangian involving the new fields is given by

$$\begin{aligned} \mathcal{L} \supset & \left(\lambda_i^Q \overline{Q'} Q_i \Phi_S + \lambda_i^U \overline{Q'} U_i \Phi_D + \lambda_i^D \overline{Q'} D_i \tilde{\Phi}_D + \lambda_i^L \overline{L'} L_i \Phi_S + \lambda_i^E \overline{L'} E_i \tilde{\Phi}_D + a_H H^\dagger \tilde{\Phi}_D \Phi_S \right. \\ & \left. + a'_H H^\dagger \tilde{\Phi}_D \Phi_S^\dagger + \frac{\lambda'_2}{2} (\tilde{\Phi}_D^\dagger H)^2 + \text{h.c.} \right) - M_Q \overline{Q'} Q' - M_L \overline{L'} L' - M_S^2 \Phi_S^* \Phi_S - M_D^2 \Phi_D^* \Phi_D \\ & + \frac{\lambda_S}{2} (\Phi_S^\dagger \Phi_S)^2 + \frac{\lambda_D}{2} (\Phi_D^\dagger \Phi_D)^2 + \lambda_{SD} |\Phi_S|^2 |\Phi_D|^2 + \lambda_{SH} |\Phi_S|^2 |H|^2 + \lambda_{DH} |\Phi_D|^2 |H|^2 \\ & + \lambda'_1 (H^\dagger \tilde{\Phi}_D) (\tilde{\Phi}_D^\dagger H), \end{aligned} \quad (3)$$

where we have systematically considered the scalar potential relative to the phenomenology that we are interested in. We denote the left-handed exotic quarks, right-handed exotic quarks, left-handed exotic leptons, right-handed exotic leptons, left-handed quark doublets, right-handed up-type quarks, right-handed down-type quarks, left-handed lepton doublets, and right-handed down-type leptons as $Q'_L, Q'_R, L'_L, L'_R, Q_i, U_i, D_i, L_i$, and E_i ($i=1,2,3$), respectively.

After the breaking of the electroweak symmetry, the terms involved λ_{SH} and λ_{DH} will contribute to masses of Φ_S and Φ_D , respectively, while the term involved a_H will induce mixing of S_s^0 and S_d^0 . For simplicity, we choose a'_H, λ'_1 and λ'_2 to be zero. Therefore, the modified mass matrix of the BSM neutral scalars can be written as

$$U^\dagger \begin{pmatrix} M_S^2 + \frac{\lambda_{SH}v^2}{2} & a_H^*v/\sqrt{2} \\ a_Hv/\sqrt{2} & M_D^2 + \frac{\lambda_{DH}v^2}{2} \end{pmatrix} U = \begin{pmatrix} M_{S_1}^2 & \\ & M_{S_2}^2 \end{pmatrix}, \quad (4)$$

where $v \simeq 246$ GeV. The corresponding mass eigenstates S_1 and S_2 have physical masses of

$$M_{S_{1,2}}^2 = \left(M_S^2 + \frac{\lambda_{SH}v^2}{2} + M_D^2 + \frac{\lambda_{DH}v^2}{2} \mp \Delta M^2 \right) / 2 \quad (5)$$

with

$$\Delta M^2 \equiv \sqrt{\left(M_D^2 + \frac{\lambda_{DH}v^2}{2} - M_S^2 - \frac{\lambda_{SH}v^2}{2} \right)^2 + 2a_H^2v^2}. \quad (6)$$

The mixing of S_1 and S_2 is given by

$$U = \begin{pmatrix} \frac{\sqrt{2}a_Hv}{\sqrt{\left(M_D^2 + \frac{\lambda_{DH}v^2}{2} - M_S^2 - \frac{\lambda_{SH}v^2}{2} - \Delta M^2 \right)^2 + 2a_H^2v^2}} & -\frac{M_D^2 + \frac{\lambda_{DH}v^2}{2} - M_S^2 - \frac{\lambda_{SH}v^2}{2} - \Delta M^2}{\sqrt{\left(M_D^2 + \frac{\lambda_{DH}v^2}{2} - M_S^2 - \frac{\lambda_{SH}v^2}{2} - \Delta M^2 \right)^2 + 2a_H^2v^2}} \\ \frac{M_D^2 + \frac{\lambda_{DH}v^2}{2} - M_S^2 - \frac{\lambda_{SH}v^2}{2} - \Delta M^2}{\sqrt{\left(M_D^2 + \frac{\lambda_{DH}v^2}{2} - M_S^2 - \frac{\lambda_{SH}v^2}{2} - \Delta M^2 \right)^2 + 2a_H^2v^2}} & \frac{\sqrt{2}a_Hv}{\sqrt{\left(M_D^2 + \frac{\lambda_{DH}v^2}{2} - M_S^2 - \frac{\lambda_{SH}v^2}{2} - \Delta M^2 \right)^2 + 2a_H^2v^2}} \end{pmatrix}. \quad (7)$$

The couplings between up and down type quarks have a relative misalignment, and we choose

$$\lambda_i^{Q_u} = \lambda_i^Q, \quad \lambda_i^{Q_d} = \sum_k \lambda_k^Q V_{ki}^*, \quad (8)$$

where V is the CKM matrix.

In our model, we impose that the lightest BSM particle is S_1 , which is the DM candidate. But the mass hierarchies between $M_{Q'}$, $M_{L'}$, and M_{S_2} are not mandatory.

III. THE UNITARITY CONSTRAINT

The partial wave amplitude of any 2→2 scattering process in the high-energy massless limit is [64],

$$a_{fi}^J = \frac{1}{32\pi} \int_{-1}^1 d\cos\theta d_{\mu_i\mu_f}^J(\theta) \mathcal{T}_{fi}(\sqrt{s}, \cos\theta) , \quad (9)$$

where θ is the scattering angle in the center of mass frame, $d_{\mu_i\mu_f}(\theta)$ is Wigner d -function, and $\mu_{i/f} = \lambda_{i_1/f_1} - \lambda_{i_2/f_2}$ with $\lambda_{i_1/2}$ and $\lambda_{f_1/2}$ standing for the helicities of initial and final particles, respectively.

The unitarity of S matrix respects $SS^\dagger = 1$. By considering elastic scattering and imposing that the intermediate states are two-particle states, the condition required by the unitarity of S matrix can be obtained. For general unitarity bound, one has

$$\text{Re}^2 [a_{ii}^J] + \left(\text{Im} [a_{ii}^J] - \frac{1}{2} \right)^2 \leq \frac{1}{4} . \quad (10)$$

At tree level, the above unitarity bound becomes

$$\left| \text{Re} \left(a_{ii}^{J, \text{tree}} \right) \right| \leq \frac{1}{2} . \quad (11)$$

To compute the unitarity bounds in the Yukawa sector, the helicity amplitude approach demonstrated in [64] is employed, and the general form is given in TABLE I. \mathcal{T} is the non-trivial part of S matrix. The absence of \mathcal{T} in $C^{(\prime)}$, $E^{(\prime)}$, and $F^{(\prime)}$ is due to the angular momentum conversation. In the massless limit, the entities in $A^{(\prime)}$ and $B^{(\prime)}$ vanish exactly since \mathcal{T} is proportional to the mass. Besides, the entity in D is present when considering the scattering of two scalars.

One can decompose the \mathcal{T} matrix into the following structure

$$\mathcal{T}_{f_1 f_2 i_1 i_2}^{\lambda_{f_1} \lambda_{f_2} \lambda_{i_1} \lambda_{i_2}}(\sqrt{s}, \theta) = \bigoplus_{\mathbf{r}} \sum_{m=s,t,u} \mathcal{T}_m^{\lambda_{f_1} \lambda_{f_2} \lambda_{i_1} \lambda_{i_2}}(\sqrt{s}, \theta) \mathcal{F}_{f_1 f_2 i_1 i_2}^{m, \mathbf{r}}(N) \mathbf{1}_{d_{\mathbf{r}}} , \quad (12)$$

where $\mathcal{T}_m^{\lambda_{f_1} \lambda_{f_2} \lambda_{i_1} \lambda_{i_2}}(\sqrt{s}, \theta)$ is the Lorentz part and $\mathcal{F}_{f_1 f_2 i_1 i_2}^{m, \mathbf{r}}(N)$ is the group factor. To obtain the partial wave amplitude, we should consider a concrete elastic scattering process which can occur in different channels and representations. Our strategy is

- 1) Considering which partial wave we are interested in;
- 2) Calculating the group factors of the corresponding elastic scattering process;
- 3) Combining Eqs. 9, 11, and 12 to obtain the constraint of unitarity on this elastic scattering process.

	$\mu_i = 0$ ++ --	$\mu_i = 0$ 00	$\mu_i = +1$ +-	$\mu_i = +\frac{1}{2} \quad \mu_i = -\frac{1}{2}$ +0 -0
$\mu_f = 0$ ++	\mathcal{T}^{++++}	A	B	C
--	$\mathcal{T}^{--++} \quad \mathcal{T}^{----}$			
$\mu_f = 0$ 00	A'	D	\mathcal{T}^{00+-}	E
$\mu_f = +1$ +-	B'	\mathcal{T}^{+-00}	\mathcal{T}^{+--+}	F
$\mu_f = +\frac{1}{2}$ +0				\mathcal{T}^{+0+0}
$\mu_f = -\frac{1}{2}$ -0	C'	E'	F'	\mathcal{T}^{-0-0}

TABLE I: Scattering matrix \mathcal{T} .

A. The unitarity constraint of λ_2^Q

According to the classification in Ref. [64], the term $\lambda_i^Q \overline{Q}' Q_i \Phi_S$ in Eq. 3 corresponds to the first model of dirac type theory with respect to $SU(3)_C$ and $SU(2)_L$. Since Q_i denotes a left-handed field, \overline{Q}' should be a right-handed field. The term for the second generation is $\lambda_2^Q \overline{Q}'_R Q_2 \Phi_S$. In the massless limit, (anti-)fermions described by the left-handed and right-handed spinors have helicities of $-\frac{1}{2}$ ($\frac{1}{2}$) and $\frac{1}{2}$ ($-\frac{1}{2}$), respectively.

1. $J = 0$ partial wave

TABLE. I shows that only \mathcal{T}^{++++} and its conjugation contribute to the $J = 0$ partial wave. Since Q'_R and \overline{Q}_2 are in the fundamental and anti-fundamental representations of $SU(2)_L$ and $SU(3)_C$, the tensor decomposition of $Q'_R \overline{Q}_2$ gives

$$++ \left\{ Q'_R \overline{Q}_2 \sim (\mathbf{1} \oplus \mathbf{Adj})_{SU(2)_L} \otimes (\mathbf{1} \oplus \mathbf{Adj})_{SU(3)_C} \right. . \quad (13)$$

The elastic scattering process is mediated by the singlet complex scalar Φ_S . Thus, only the channel of the $\mathbf{1}$ representation of $SU(2)_L \times SU(3)_C$ is present. As for the group factor of this process, we have

$$++++ \left\{ \mathcal{F}_{Q'_R \overline{Q}_2 Q'_R \overline{Q}_2}^{s,1} = ---- \left\{ \mathcal{F}_{\overline{Q}'_R Q_2 \overline{Q}'_R Q_2}^{s,1} = N_2 \times N_3 = 2 \times 3 \right. , \quad (14)$$

where N comes from that both fermions involved are in the (anti-)fundamental representation of the $SU(N)$ group (there are more details in Appendix A) which means that $N_2 = 2$

and $N_3 = 3$ in our case. In the basis of $(Q'_R \bar{Q}_2, \bar{Q}'_R Q_2)$, based on Eqs. 9 and 12, we get

$$\begin{aligned}
a_{SU(3)=1, SU(2)=1}^{J=0} &= \frac{\lambda_2^Q}{32\pi} \int_{-1}^{+1} d\cos\theta d_{00}^0(\theta) \begin{pmatrix} N_2 N_3 \mathcal{T}_s^{++++} & 0 \\ 0 & N_2 N_3 \mathcal{T}_s^{----} \end{pmatrix} \\
&= \frac{\lambda_2^Q}{32\pi} \int_{-1}^{+1} d\cos\theta \begin{pmatrix} 2 \times 3 \times (-1) & 0 \\ 0 & 2 \times 3 \times (-1) \end{pmatrix} \\
&= -\frac{3\lambda_2^Q}{8\pi}, \tag{15}
\end{aligned}$$

where the last step means that we find the largest eigenvalue after the diagonalization of the matrix. Besides, we have used $d_{00}^0(\theta) = 1$ and $\mathcal{T}_s^{++++} = \mathcal{T}_s^{----} = -1$ according to Table 2 in [64]. Then, the perturbation unitarity condition of Eq. 11 leads to the bound

$$|\lambda_2^Q| \leq 2.05. \tag{16}$$

B. A brief summary of the unitarity constraints in Yukawa sector

The elaborate constraints on the parameters of Yukawa sector in our model are given in TABLE II, and the details can be found in Appendix A.

	$(Q'_R \bar{Q}_2, \bar{Q}'_R Q_2)$	$(Q'_R \bar{Q}_3, \bar{Q}'_R Q_3)$	$(L'_R \bar{L}_2, \bar{L}'_R L_2)$	$(\bar{L}'_L E, L'_L \bar{E})$
$J = 0$	$ \lambda_2^Q \leq 2.05$	$ \lambda_3^Q \leq 2.05$	$ \lambda_2^L \leq 3.54$	$ \lambda_2^E \leq 5.01$
Base I	$(\bar{Q}_2 \Phi_S^*, Q_2 \bar{\Phi}_s^*)$	$(\bar{Q}_3 \Phi_S^*, Q_3 \bar{\Phi}_s^*)$	$(L'_R \Phi_S^*, \bar{L}'_R \Phi_S)$	$(E \tilde{\Phi}_D, \bar{E} \tilde{\Phi}_D^*)$
$J = \frac{1}{2}$	$ \lambda_2^Q \leq 5.01$	$ \lambda_3^Q \leq 5.01$	$ \lambda_2^L \leq 5.01$	$ \lambda_2^E \leq 7.09$
Base II	$(Q'_R \Phi_s^*, \bar{Q}'_R \Phi_s)$	$(Q'_R \Phi_s^*, \bar{Q}'_R \Phi_s)$	$(\bar{L}_2 \Phi_S^*, L_2 \Phi_S)$	$(\bar{L}'_L \tilde{\Phi}_D, L'_L \tilde{\Phi}_D^*)$
$J = \frac{1}{2}$	$ \lambda_2^Q \leq 5.01$	$ \lambda_3^Q \leq 5.01$	$ \lambda_2^L \leq 5.01$	$ \lambda_2^E \leq 5.01$

TABLE II: Unitarity constraint in Yukawa sector.

For λ_2^Q , λ_3^Q and λ_2^L , the strict constraints come from $J = 0$ partial wave, which are $|\lambda_2^Q| \leq 2.05$, $|\lambda_3^Q| \leq 2.05$ and $|\lambda_2^L| \leq 3.54$. While the $J = \frac{1}{2}$ partial wave leads to a relative weaker bound. For λ_2^E , the $J = 0$ partial wave gives the strict bound $|\lambda_2^E| \leq 5.01$ as well, however, $J = \frac{1}{2}$ partial wave in an alternative base $(\bar{L}'_L \tilde{\Phi}_D, L'_L \tilde{\Phi}_D^*)$ leads to the same bound.

The unitarity constraints on Yukawa couplings eventually lead the following bounds

$$\begin{aligned}
|\lambda_2^Q| &\leq 2.05 , \\
|\lambda_3^Q| &\leq 2.05 , \\
|\lambda_2^L| &\leq 3.54 , \\
|\lambda_2^E| &\leq 5.01 .
\end{aligned} \tag{17}$$

Of course, we need to consider the perturbative bounds on the Yukawa couplings, *i.e.*, all the Yukawa couplings are smaller than $\sqrt{4\pi}$.

IV. THE TENTATIVE NEW PHYSICS ANOMALIES AND DARK MATTER

In this Section, we will address the R_K and B_s mixing, muon $g - 2$, and dark matter relic density simultaneously. Random scan of the model parameters is employed, and the benchmark points satisfying all the current constraints are selected.

A. R_K and B_s mixing

According to [61], the contribution to R_K can be described by the following effective Lagrangian,

$$\mathcal{H}_{\text{eff}}^{bs\mu\mu} \supset -\mathcal{N} \left[C_9^{bs\mu\mu} (\bar{s}\gamma_\mu P_L b) (\bar{\mu}\gamma^\mu \mu) + C_{10}^{bs\mu\mu} (\bar{s}\gamma_\mu P_L b) (\bar{\mu}\gamma^\mu \gamma_5 \mu) + \text{h.c.} \right] , \tag{18}$$

where the normalization is given by

$$\mathcal{N} \equiv \frac{4G_F}{\sqrt{2}} \frac{e^2}{16\pi^2} V_{tb} V_{ts}^* . \tag{19}$$

Contributions to $C_{9,10}^{bs\mu\mu}$ from the BSM particles are

$$\Delta C_9^{bs\mu\mu} = -\frac{\lambda_3^{Q_d} \lambda_2^{Q_d*}}{128\pi^2 \mathcal{N}} \sum_{\alpha=1,2} \frac{|U_{1\alpha}|^4 |\lambda_2^L|^2 + |U_{1\alpha}|^2 |U_{2\alpha}|^2 |\lambda_2^E|^2}{M_{S_\alpha}^2} F_2 \left(\frac{M_Q^2}{M_{S_\alpha}^2}, \frac{M_L^2}{M_{S_\alpha}^2} \right) , \tag{20}$$

$$\Delta C_{10}^{bs\mu\mu} = \frac{\lambda_3^{Q_d} \lambda_2^{Q_d*}}{128\pi^2 \mathcal{N}} \sum_{\alpha=1,2} \frac{|U_{1\alpha}|^4 |\lambda_2^L|^2 - |U_{1\alpha}|^2 |U_{2\alpha}|^2 |\lambda_2^E|^2}{M_{S_\alpha}^2} F_2 \left(\frac{M_Q^2}{M_{S_\alpha}^2}, \frac{M_L^2}{M_{S_\alpha}^2} \right) , \tag{21}$$

with loop function

$$F_2(x, y) \equiv \frac{1}{(x-1)(y-1)} + \frac{x^2 \log x}{(x-1)^2(x-y)} + \frac{y^2 \log y}{(y-1)^2(y-x)} . \tag{22}$$

According to the up-to-date fitting [4] (2σ), the contribution to LFU violation in $b \rightarrow s\mu\mu$ from $\Delta C_9^{bs\mu\mu}$ and $\Delta C_{10}^{bs\mu\mu}$ needs to satisfy

$$6.74 + 9.04(\Delta C_9^{bs\mu\mu})^2 + \Delta C_9^{bs\mu\mu}(14.96 - 10.68\Delta C_{10}^{bs\mu\mu}) + \Delta C_{10}^{bs\mu\mu}(-13.22 + 11.90\Delta C_{10}^{bs\mu\mu}) \leq 1. \quad (23)$$

The contribution to $B_s - \bar{B}_s$ oscillation can be induced from the following operators

$$\mathcal{H}_{\text{eff}}^{bd_i} \supset C_1^{bd_i} (\bar{d}_i \gamma_\mu P_L b) (\bar{d}_i \gamma^\mu P_L b) + \text{h.c.} \quad d_i = d, s. \quad (24)$$

The $Q' - \Phi_S$ box diagram gives Wilson coefficients

$$\Delta C_1^{bd_i} = \frac{(\lambda_3^{Q_d} \lambda_i^{Q_d^*})^2}{128\pi^2} \sum_{\alpha=1,2} \frac{|U_{1\alpha}|^4}{M_{S_\alpha}^2} F\left(\frac{M_Q^2}{M_{S_\alpha}^2}\right), \quad (25)$$

where the loop function is

$$F(x) \equiv \frac{x^2 - 1 - 2x \log x}{(x - 1)^3}. \quad (26)$$

The bound given in [10, 11] is

$$\Delta C_1^{bs} < 2.1 \times 10^{-5} \text{TeV}^{-2}. \quad (27)$$

B. Muon g-2

The contribution of BSM particles in this model to a_μ is

$$\Delta a_\mu \approx -\frac{m_\mu M_L}{8\pi^2} \sum_{\alpha=1,2} \frac{\text{Re}(\lambda_2^L \lambda_2^{E*} U_{1\alpha} U_{2\alpha}^*)}{M_{S_\alpha}^2} f_{LR}\left(\frac{M_L^2}{M_{S_\alpha}^2}\right), \quad (28)$$

where the loop function is

$$f_{LR}(x) \equiv \frac{3 - 4x + x^2 + 2 \log x}{2(x - 1)^3}. \quad (29)$$

The latest (1σ) discrepancy is given by [9]

$$a_\mu^{\text{EXP}} - a_\mu^{\text{SM}} = (2.51 \pm 0.59) \times 10^{-9}. \quad (30)$$

C. Dark matter phenomenology

We consider the lightest neutral scalar S_1 as the DM candidate, and the typical freeze-out mechanism controls the DM production. In addition, the annihilation and co-annihilation processes can deplete the DM relic density.

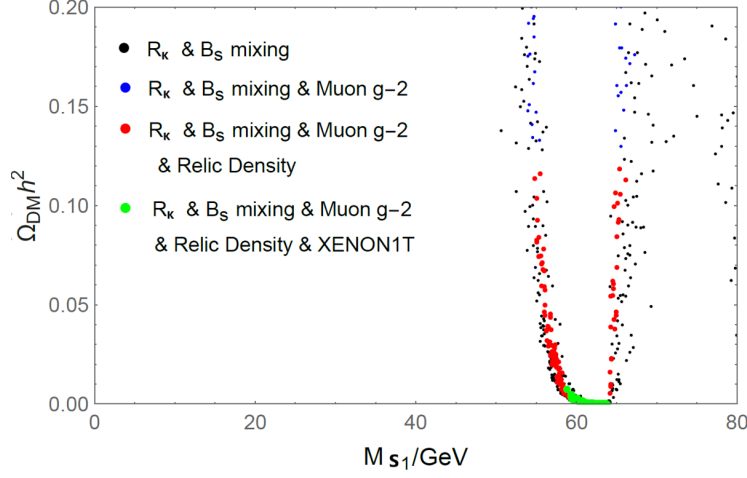


FIG. 1: DM annihilation mediated by Higgs resonance. The black points satisfy the constraints of R_K (2σ) and $B_s - \bar{B}_s$, the blue points satisfy the constraints of R_K (2σ), $B_s - \bar{B}_s$ and muon g-2, the red points satisfy the constraints of R_K (2σ), $B_s - \bar{B}_s$, muon g-2 and DM relic density, and the green points satisfy the constraints of R_K (2σ), $B_s - \bar{B}_s$, muon g-2, DM relic density and XENON1T direct detection.

In our random scan, the ranges of parameters have to satisfy the bounds of unitarity given in TABLE II. In addition, we set the couplings to the right-handed quarks (λ_i^U and λ_i^D) and the left-handed quarks of the first generation (λ_1^Q) to be zero, and only consider the second family couplings in the lepton sector (λ_2^L and λ_2^E). The elaborate scan ranges of parameters are given in TABLE III.

Parameters	λ_2^Q	λ_3^Q	λ_2^L	λ_2^E	a_H/TeV	$\lambda_S/2$	$\lambda_D/2$
Range	[-2,2]	[-2,2]	[-3,3]	[-3,3]	[-1,1]	[-3,3]	[-3,3]
Parameters	M_S/TeV	M_D/TeV	$M_{L'}/\text{TeV}$	$M_{Q'}/\text{TeV}$	λ_{SH}	λ_{DH}	λ_{SD}
Range	[0,2]	[0,5]	[0.11,5]	[1.2,6]	[-1,1]	[-1,1]	[-3,3]

TABLE III: The scan ranges of parameters employed in the random scan. New parameters of this model which are not shown in this table are set to be zero.

FIG. 1 shows the DM relic density versus the mass of S_1 . The conditions from R_K (2σ) and $B_s - \bar{B}_s$ (black dot), the muon g-2 (1σ) constraint (blue dot), the constraint of (rescaled) DM relic density (red dot), and the constraint from XENON1T experiment (green dot) are applied in order. It can be seen from FIG. 1 that the Higgs mediated DM annihilation

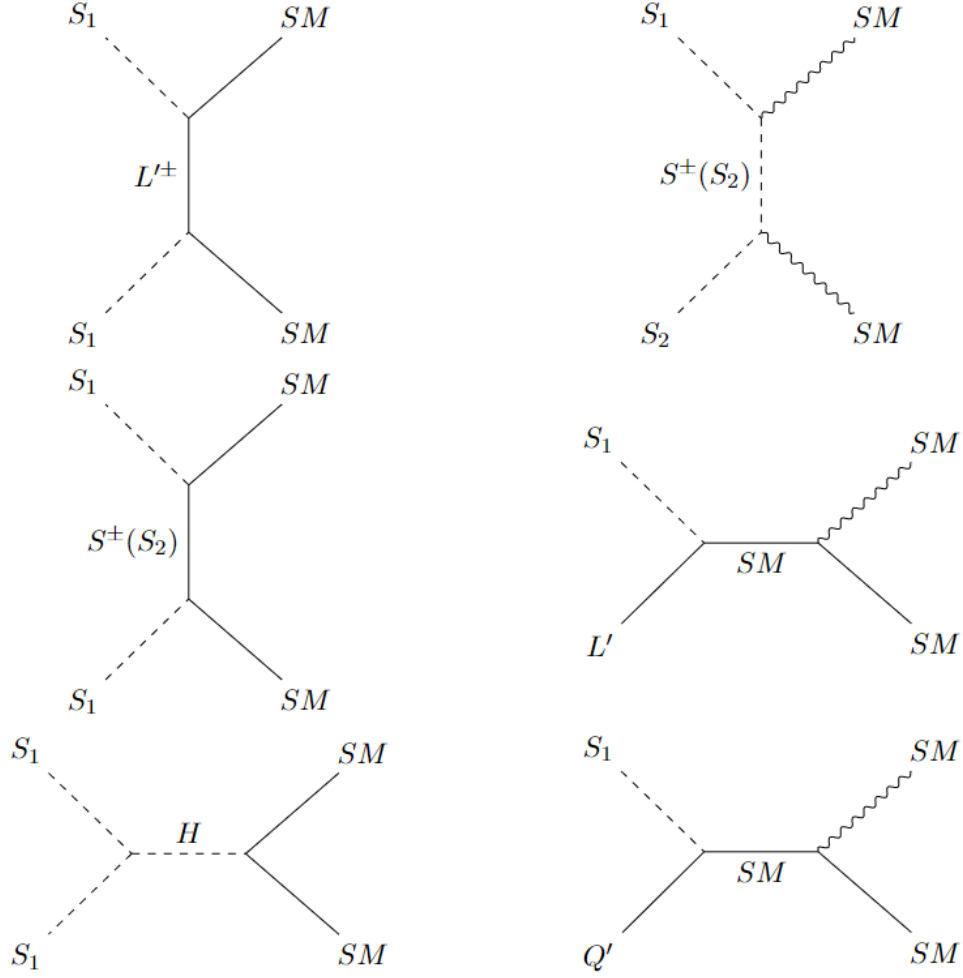


FIG. 2: The DM (co-)annihilation processes.

channel efficiently depletes the DM, leading to the minimum value of relic density.

The DM relic density is controlled by the (co-)annihilation processes shown in FIG. 2.

- 1) Annihilation of two S_1 will always happen no matter what the mass differences between S_1 and other particles are, which are demonstrated in the first column of FIG. 2. The annihilation process mediated by the Higgs boson shown in the last diagram of the first column of FIG. 2 can efficiently deplete the DM relic density.
- 2) Co-annihilations of S_1 and other particles (S_2 , L' , and Q') will occur when their mass difference are small, which are shown in the second column of FIG. 2.

Ten benchmark points are given in TABLE IV, and all these points can evade the experimental constraints from R_K and B_s mixing, and muon g-2. Points 1 and 2 correspond to

annihilation of two S_1 . The Higgs mediated DM annihilation is demonstrated by Points 3 and 4. Point 5 (6), Point 7 (8), and Point 9 (10) are characterized by the co-annihilation between S_1 and S_2 , L' , and Q' , respectively. In addition, the dark matter candidate S_1 can explain some of the observed relic density and evade XENON1T experiment as well.

	Point 1	Point 2	Point 3	Point 4	Point 5	Point 6	Point 7	Point 8	Point 9	Point 10
Relic density	0.011522	0.093819	0.000076	0.000046	0.011026	0.01447	0.017495	0.016008	0.04798	0.048167
λ_2^Q	0.10101	0.5996	-0.12509	-0.13069	1.1424	1.3606	0.54168	0.55338	0.22722	0.26312
λ_3^Q	-1.1951	-1.0286	1.8403	1.7261	-1.0692	-0.48519	-1.3764	-1.2747	-1.226	-1.2927
λ_2^L	-2.6267	-2.9421	1.9734	1.9598	2.9536	2.9733	-2.492	-2.4106	-2.7338	-2.7466
λ_2^E	0.58956	-1.1191	0.18295	0.17041	1.2603	1.3269	-1.9362	-1.9258	-1.5627	-1.5474
a_H/GeV	-269.33	105.49	241.84	239.07	77.867	193.76	46.396	48.413	250.22	199.99
$\lambda_S/2$	-2.93125	0.88935	0.05591	0.065355	-2.36415	1.4342	-1.2625	-1.3191	-2.0845	-2.08535
$\lambda_D/2$	-2.8127	1.41265	0.25705	0.276025	1.3104	-2.75535	-1.44125	-1.4204	0.52185	0.470945
λ_{SH}	0.60612	0.03331	0.00091576	0.0014208	0.00071561	0.0003719	-0.00022894	-0.00022618	0.00081559	-0.00048164
λ_{DH}	0.70071	-0.68513	0.0011148	0.0026438	0.00087688	-0.00080729	0.00079511	0.0007723	-0.00078335	0.00096566
λ_{SD}	-0.018352	0.36301	0.20188	0.23401	-1.8201	1.2962	-2.5734	-2.5342	2.5104	2.4429
M_S/GeV	570.9	506.36	69.768	71.562	1240.6	1065.4	1138	1105.3	1285.9	1273.8
M_D/GeV	4246.1	1828.5	1385.2	1214.9	1245.6	1096.6	1723.7	1655.3	3126.3	3159.6
$M_{L'}/\text{GeV}$	825.16	1529.5	961.08	966.61	1627	2743.7	1155.1	1116.3	1682.8	1654.6
$M_{Q'}/\text{GeV}$	1726	4630.8	1987	1922.7	5986.8	3741.7	4368.4	4432.1	1295.4	1295.1
M_{S_1}/GeV	586.66	507.25	63.004	63.145	1237.1	1058.8	1138	1105.2	1285.8	1273.8
M_{S_2}/GeV	4248.6	1822.8	1385.6	1215.4	1249.1	1102.9	1723.7	1655.3	3126.3	3159.6

TABLE IV: Benchmark points in DM annihilation and co-annihilation.

In addition, we investigate the large mixing and relative small coupling case. We can see from Eqs. 20 and 21, ΔC_9 and ΔC_{10} are quadratically depended in λ_2^L . To reduce the λ_2^L , one needs small M_Q and M_L , which are already near the lower edge of experimental search. After a somehow simple analysis, one cannot have a small λ_2^L to account for all the aforementioned anomalies. In the left panel of FIG. 3, we can see that only Higgs resonance can explain the R_K , B_s mixing, muon $g-2$, and the saturated DM relic density. The right panel of FIG. 3 shows the S_1 and L' co-annihilation process with large mixing ($a_H = 500$ GeV). In this case, the R_K , B_s mixing, and muon $g-2$ can be explained simultaneously and the DM relic density is undersaturated. In FIG. 4 we display viable parameter space with different a_H . In top left panel, the flavor observables and DM relic density can be explained as well. As a_H increases, the DM relic density is undersaturated while the constraints of flavour observables are satisfied.

We intend to give some comments on the parameter space on the edge of unitarity.

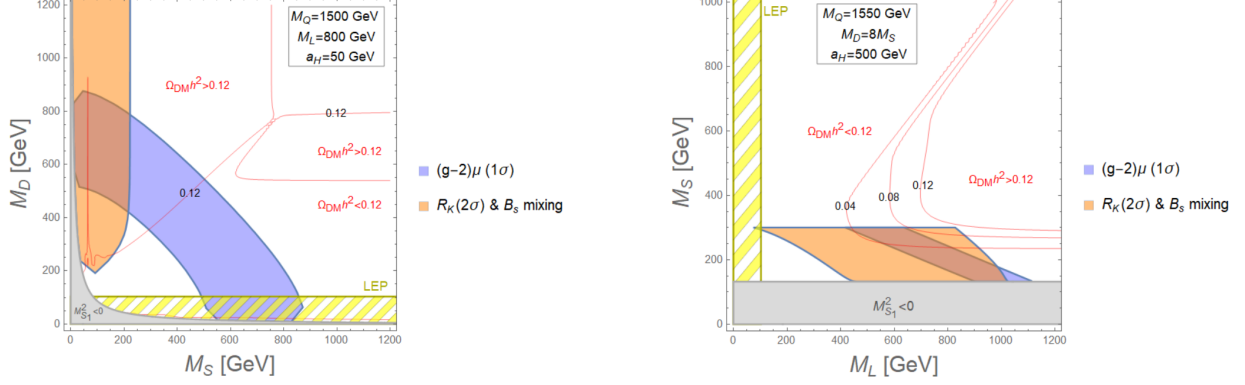


FIG. 3: The combined constraints on the M_S versus M_D plane and M_L versus M_S plane. The couplings are $\lambda_2^Q = 0.49$, $\lambda_3^Q = -0.49$, $\lambda_2^L = 1.4$, $\lambda_2^E = -0.4$, $\lambda_{SH} = \lambda_{DH} = 0.001$ (left), $\lambda_2^Q = 0.49$, $\lambda_3^Q = -0.49$, $\lambda_2^L = 1.5$, $\lambda_2^E = -0.06$, $\lambda_{SH} = \lambda_{DH} = 0.001$ (right).

In FIG. 5 we employ the conservative parameters which are consistent with the unitarity bounds in Eq. 17 and avoid large quantum corrections. Roughly speaking, we find the upper bounds on the masses of exotic particles, $M_{Q'} = 17.5$ TeV and $M_{L'} = 2.4$ TeV which can account for the R_K , B_s mixing, muon $g - 2$, and the saturated DM relic density.

V. W BOSON MASS

The oblique corrections contributing to W boson mass are given by [65, 66]

$$m_W^2 = m_W^2(SM) + \frac{\alpha c^2}{c^2 - s^2} m_Z^2 \left[-\frac{1}{2} \Delta S + c^2 \Delta T + \frac{c^2 - s^2}{4s^2} \Delta U \right], \quad (31)$$

where α is the fine structure constant, $c = \cos\theta_W$, $s = \sin\theta_W$. The expressions of ΔS and ΔT are

$$\Delta S = \frac{1}{2\pi} \left[\frac{1}{6} \log \left(\frac{m_R^2}{m_{S^\pm}^2} \right) - \frac{5}{36} + \frac{m_R^2 m_A^2}{3(m_A^2 - m_R^2)^2} + \frac{m_A^4 (m_A^2 - 3m_R^2)}{6(m_A^2 - m_R^2)^3} \log \left(\frac{m_A^2}{m_R^2} \right) \right], \quad (32)$$

$$\Delta T = \frac{1}{32\pi^2 \alpha v^2} [F(m_{S^\pm}^2, m_A^2) + F(m_{S^\pm}^2, m_R^2) - F(m_A^2, m_R^2)], \quad (33)$$

with the loop function

$$F(x, y) = \begin{cases} \frac{x+y}{2} - \frac{xy}{x-y} \log \left(\frac{x}{y} \right), & x \neq y \\ 0, & x = y \end{cases}, \quad (34)$$

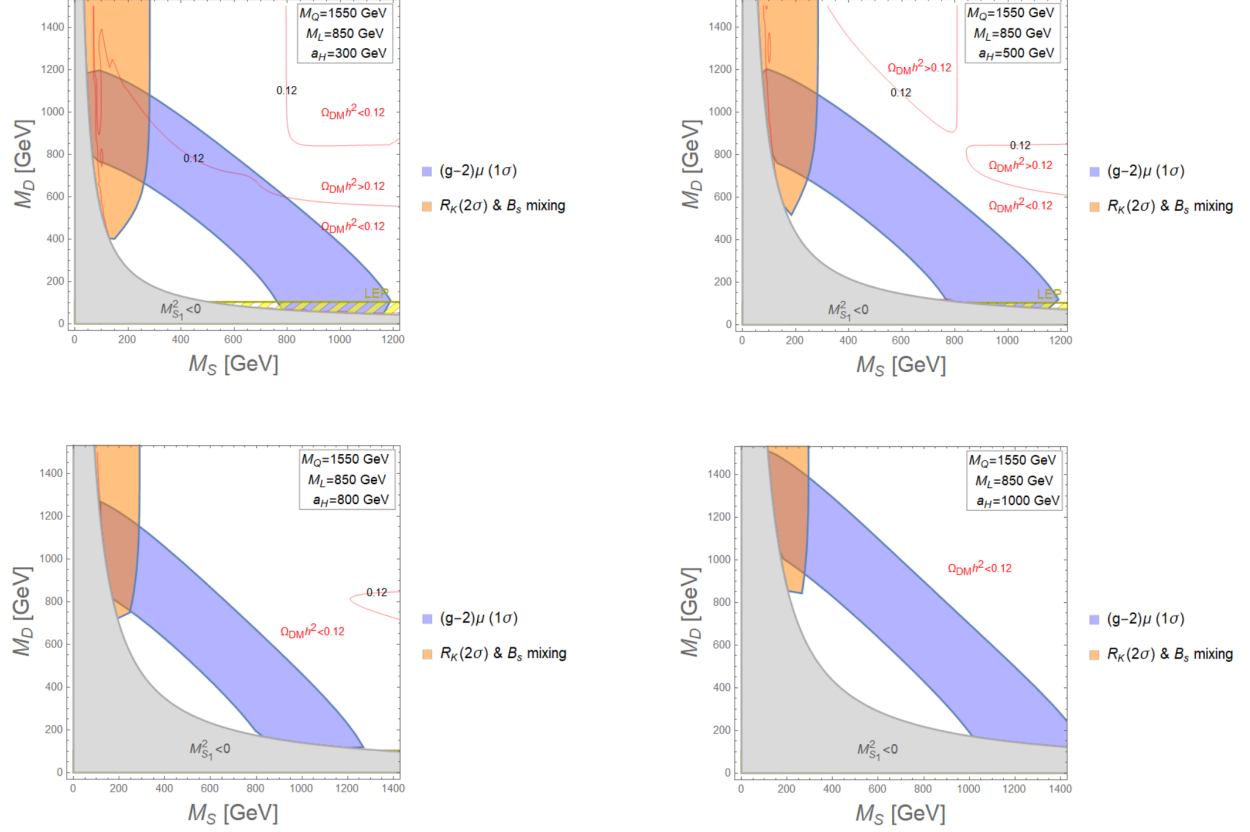


FIG. 4: The combined constraints on M_S and M_D plane with different a_H . The couplings are setting as $\lambda_2^L = 1.5$, $\lambda_2^Q = 0.49$, $\lambda_3^Q = 0.49$, $\lambda_{SH} = \lambda_{DH} = 0.001$ and λ_2^E are -0.1, -0.06, -0.04, -0.04 respectively

where we ignore ΔU and rewrite the scalar doublet as

$$\Phi_D = \begin{pmatrix} S_d^0 = R + iA \\ S^- \end{pmatrix} \quad (35)$$

For convenience, we consider the small mixing between scalar singlet and doublet. To interpret the W boson mass anomaly, the scalar potential is essential to give an appropriate mass splitting between neutral and charge part of the doublet. We find that W boson mass cannot be explained if we consider λ'_2 only. However, if the λ_{DH} , λ'_2 , λ'_1 are involved simultaneously, the W mass anomaly can be accounted for in a straightforward way. We can fit the up-to-date measurement of W boson mass (1σ) by using Eqs. 31, 32 and 33. FIG.6 shows the corresponding oblique parameters between ΔS and ΔT , and the mass splitting between neutral and charge part of the scalar doublet.

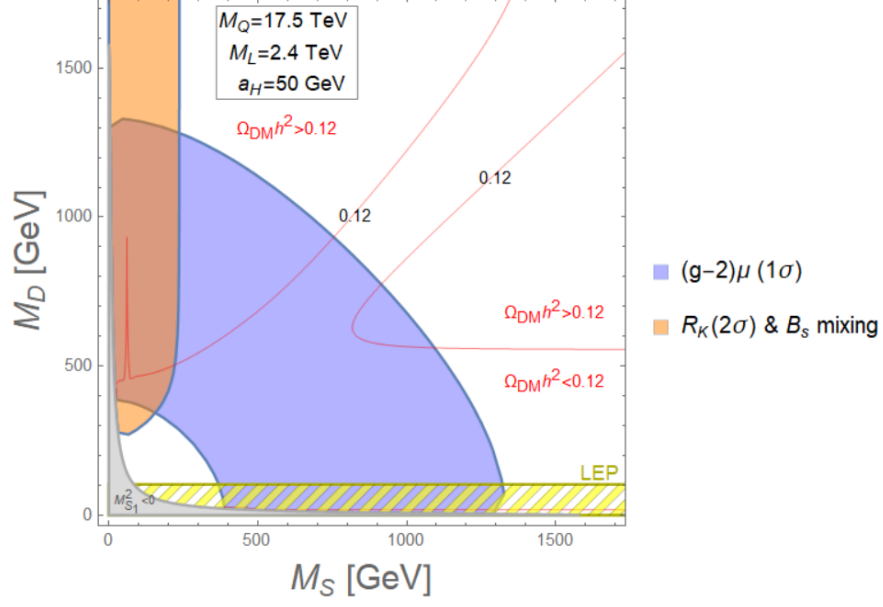


FIG. 5: The parameter space consistent with unitarity bounds. The couplings are setting as $\lambda_2^L = 2.9$, $\lambda_2^E = -2.9$, $\lambda_2^Q = 1.4$, $\lambda_3^Q = -2.0$, $\lambda_{SH} = \lambda_{DH} = 0.001$

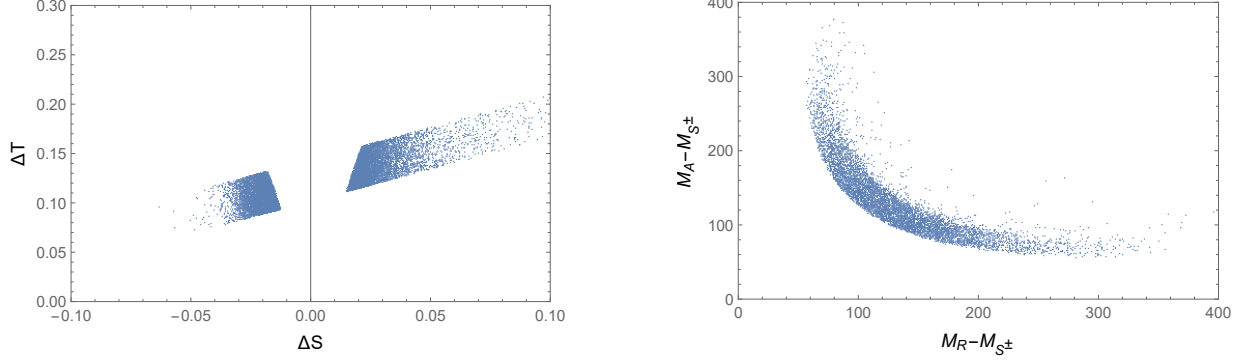


FIG. 6: The points that explain the up-to-date W boson mass (1σ) in ΔS versus ΔT plane (left) and the mass splitting between neutral and charged part of the scalar doublet plane (right).

VI. CONCLUSION

We have revisited the SESM which can address various tentative new physics anomalies and DM. The mass splitting between the charged and neutral parts of scalar doublet via scalar potential can account for the W boson mass anomaly. Moreover, we considered the unitarity constraints in the Yukawa sector. Also, we employed the random scan approach,

and obtained the viable parameter spaces which can explain the B physics anomaly, muon anomalous magnetic moment, W mass anomaly, and dark matter relic density simultaneously. To be concrete, we select some benchmark points. The various DM (co)-annihilation and resonance processes are investigated, and the benchmark points whose DM relic density are around or smaller than the observed DM relic density are demonstrated. In particular, the Higgs pole, S_1 and S_1 annihilation, S_1 and S_2 , L' , Q' co-annihilation are demonstrated as well, and all these points can evade the current flavor and XENON1T direct detection constraints.

ACKNOWLEDGMENTS

We would like to thank Lorenzo Calibbi very much for the helpful discussions. This work is supported in part by the National Key Research and Development Program of China Grant No. 2020YFC2201504, by the Projects No. 11875062, No. 11947302, and No. 12047503 supported by the National Natural Science Foundation of China, as well as by the Key Research Program of the Chinese Academy of Sciences, Grant NO. XDPB15.

Appendix A: The Unitarity Constraint on λ_2^Q

1. The Unitarity Constraint on λ_2^Q

a. $J = 0$ Partial Wave

Two particle system is defined as

$$\begin{aligned} |\psi\bar{\psi}\rangle_1 &= \frac{1}{\sqrt{N}} \delta_a^b |\psi_a \bar{\psi}^b\rangle, \\ |\psi\bar{\psi}\rangle_{\text{Adj}}^A &= \sqrt{2} (T^A)_a^{\cdot b} |\psi_a \bar{\psi}^b\rangle, \\ |\psi\psi\rangle_{\mathbf{S}}^A &= (T_{\mathbf{S}}^A)_{ab} |\psi_a \psi_b\rangle. \end{aligned} \tag{A1}$$

The group factor can be caculate as follows

$$\begin{aligned} \langle\psi\bar{\psi}|\psi\bar{\psi}\rangle_1 &= \langle\psi_c \bar{\psi}^d| \frac{1}{\sqrt{N}} \delta_c^d \frac{1}{\sqrt{N}} \delta_a^b |\psi_a \bar{\psi}^b\rangle \\ &= \frac{N}{\sqrt{N}} \frac{N}{\sqrt{N}} \langle\psi_1 \bar{\psi}_1|\psi_1 \bar{\psi}_1\rangle \\ &= N \langle\psi_1 \bar{\psi}_1|\psi_1 \bar{\psi}_1\rangle, \end{aligned} \tag{A2}$$

where $\langle \psi \bar{\psi} | \psi \bar{\psi} \rangle_1$ denotes the elastic scattering process in singlet channel, and ψ_1 stands for one component of ψ in the fundamental representation.

b. $J = \frac{1}{2}$ Partial Wave

$\mathcal{T}^{+0^*+0^*}$ and \mathcal{T}^{-0-0} contribute to $J = \frac{1}{2}$ partial wave as follows

$$+0^* \left\{ \bar{Q}_2 \Phi_S^* \sim \bar{\square} \right. . \quad (\text{A3})$$

The one fermion and one scalar state is

$$|\Psi S\rangle = 1|\Psi S\rangle , \quad (\text{A4})$$

with group factor

$$\langle \Psi S | \Psi S \rangle = 1 \langle \Psi S | \Psi S \rangle . \quad (\text{A5})$$

We have $+0^* + 0^*$ or $-0 - 0$ $\left\{ \mathcal{F}_{\bar{Q}_2 \Phi_S^* \bar{Q}_2 \Phi_S^*}^{u, \bar{\square}} = \mathcal{F}_{Q_2 \Phi_S^* Q_2 \Phi_S^*}^{u, \square} = 1 \right.$. In $(\bar{Q}_2 \Phi_S^*, Q_2 \bar{\Phi}_s^*)$ basis, we have (Note that the base $(Q'_R \Phi_s^*, \bar{Q}'_R \Phi_s)$ leads to the same result.)

$$\begin{aligned} a_{SU(3)=\bar{\square} \text{ or } \square, SU(2)=\bar{\square} \text{ or } \square}^{J=1/2} &= \frac{\lambda_2^{Q^2}}{32\pi} \int_{-1}^{+1} d \cos \theta d^{\frac{1}{2} \frac{1}{2}}_{\frac{1}{2} \frac{1}{2}}(\theta) \begin{pmatrix} \mathcal{T}_u^{+0^*+0^*} & 0 \\ 0 & \mathcal{T}_u^{-0-0} \end{pmatrix} \\ &= \frac{\lambda_2^{Q^2}}{32\pi} \int_{-1}^{+1} d \cos \theta \cos \frac{\theta}{2} \begin{pmatrix} -\frac{1}{\cos \frac{\theta}{2}} & 0 \\ 0 & -\frac{1}{\cos \frac{\theta}{2}} \end{pmatrix} \\ &= -\frac{\lambda_2^{Q^2}}{16\pi} . \end{aligned} \quad (\text{A6})$$

This corresponds to the bound

$$|\lambda_2^Q| \leq 5.01 . \quad (\text{A7})$$

2. The Unitarity Constraint on λ_3^Q

The λ_3^Q in Eq. 3 is the first model of dirac type theory in both $SU(3)_C$ and $SU(2)_L$ as well, and thus the constraint on λ_3^Q is exact the same as λ_2^Q . We have the strict bound $|\lambda_3^Q| \leq 2.05$ from $J = 0$ partial wave.

3. The Unitarity Constraint on λ_2^L

As we have claimed in the quark sector before, the Lagrangian becomes $\lambda_i^L \bar{L}' L_i \Phi_S \rightarrow \lambda_2^L \bar{L}'_R L_2 \Phi_S$. This kind of interaction can be classified by the first type of dirac theory in $SU(2)_L$.

a. $J = 0$ Partial Wave

One can consider the elastic scatting processes $L'_R \bar{L}_2 \rightarrow L'_R \bar{L}_2$ or $\bar{L}'_R L_{2L} \rightarrow \bar{L}'_R L_2$. Group factor is $++++$ or $----$ $\left\{ \mathcal{F}_{L'_R \bar{L}_2 L'_R \bar{L}_2}^{s,1} = \mathcal{F}_{\bar{L}'_R L_{2L} \bar{L}'_R L_2}^{s,1} = N \right.$.

In $(L'_R \bar{L}_2, \bar{L}'_R L_2)$ basis, we have

$$\begin{aligned} a_{SU(2)=1}^{J=0} &= \frac{\lambda_2^{L^2}}{32\pi} \int_{-1}^{+1} d\cos\theta d_{00}^0(\theta) \begin{pmatrix} N_2 \mathcal{T}_s^{++++} & 0 \\ 0 & N_2 \mathcal{T}_s^{----} \end{pmatrix} \\ &= \frac{\lambda_2^{L^2}}{32\pi} \int_{-1}^{+1} d\cos\theta \begin{pmatrix} 2 \times (-1) & 0 \\ 0 & 2 \times (-1) \end{pmatrix} \\ &= -\frac{\lambda_2^{L^2}}{8\pi}, \end{aligned} \quad (A8)$$

which gives the bound

$$|\lambda_2^L| < 3.54. \quad (A9)$$

b. $J = \frac{1}{2}$ Partial Wave

Consider the elastic scatting process $L'_R \Phi_S^* \rightarrow L'_R \Phi_S^*$ or $\bar{L}'_R \Phi_S \rightarrow \bar{L}'_R \Phi_S$, group factor is $+0^*+0^*$ or $-0-0$ $\left\{ \mathcal{F}_{L'_R \Phi_S^* L'_R \Phi_S^*}^{s,\square} = \mathcal{F}_{\bar{L}'_R \Phi_S \bar{L}'_R \Phi_S}^{s,\bar{\square}} = 1 \right.$. In $(L'_R \Phi_S^*, \bar{L}'_R \Phi_S)$ basis, we get (the basis $(\bar{L}_2 \Phi_S^*, L_2 \Phi_S)$ gives the same result.)

$$\begin{aligned} a_{SU(2)=\square \text{ or } \bar{\square}}^{J=1/2} &= \frac{\lambda_2^{L^2}}{32\pi} \int_{-1}^{+1} d\cos\theta d_{\frac{1}{2}\frac{1}{2}}^{\frac{1}{2}}(\theta) \begin{pmatrix} \mathcal{T}_u^{+0^*+0^*} & 0 \\ 0 & \mathcal{T}_u^{-0-0} \end{pmatrix} \\ &= \frac{\lambda_2^{L^2}}{32\pi} \int_{-1}^{+1} d\cos\theta \cos\frac{\theta}{2} \begin{pmatrix} -\frac{1}{\cos\frac{\theta}{2}} & 0 \\ 0 & -\frac{1}{\cos\frac{\theta}{2}} \end{pmatrix} \\ &= -\frac{\lambda_2^{L^2}}{16\pi}, \end{aligned} \quad (A10)$$

with the relatively weak bound

$$|\lambda_2^L| < 5.01. \quad (A11)$$

4. The Unitarity Constraint on λ_2^E

The Lagrangian is given by $\lambda_i^E \bar{L}' E_i \tilde{\Phi}_D \rightarrow \lambda_2^E \bar{L}'_L E_2 \tilde{\Phi}_D$. Since E is the $SU(2)_L$ singlet and Φ_D is $SU(2)_L$ doublet, this kind of interaction can be classified into the second type of dirac theory.

a. $J = 0$ Partial Wave

Two particle state is defined (E is $SU(2)_L$ singlet fermion) as

$$|\bar{L}'_L E\rangle_{\square}^a = |\bar{L}'^a_L E\rangle . \quad (\text{A12})$$

The group factor is

$$\langle \bar{L}'^a_L E | \bar{L}'^a_L E \rangle = 1 \langle \bar{L}'^a_L E | \bar{L}'^a_L E \rangle . \quad (\text{A13})$$

We have $++++$ or $----$ $\left\{ \mathcal{F}_{\bar{L}'_L E \bar{L}'_L E}^{s, \square} = \mathcal{F}_{L'_L \bar{E} L'_L \bar{E}}^{s, \square} = 1 \right.$

In $(\bar{L}'_L E, L'_L \bar{E})$ basis, we have

$$\begin{aligned} a_{SU(2)=\square \text{ or } \square}^{J=0} &= \frac{\lambda_2^{E^2}}{32\pi} \int_{-1}^{+1} d \cos \theta d_{00}^0(\theta) \begin{pmatrix} \mathcal{T}_s^{++++} & 0 \\ 0 & \mathcal{T}_s^{----} \end{pmatrix} \\ &= \frac{\lambda_2^{E^2}}{32\pi} \int_{-1}^{+1} d \cos \theta \begin{pmatrix} -1 & 0 \\ 0 & -1 \end{pmatrix} \\ &= -\frac{\lambda_2^{E^2}}{16\pi} , \end{aligned} \quad (\text{A14})$$

with unitarity bound

$$|\lambda_2^E| < 5.01 . \quad (\text{A15})$$

b. $J = \frac{1}{2}$ Partial Wave

Group factor is $+0 + 0$ or $-0^* - 0^*$ $\left\{ \mathcal{F}_{E\tilde{\Phi}_D E\tilde{\Phi}_D}^{s,\square} = \mathcal{F}_{\bar{E}\tilde{\Phi}_D^* \bar{E}\tilde{\Phi}_D^*}^{s,\square} = 1 \right.$. In $(E\tilde{\Phi}_D, \bar{E}\tilde{\Phi}_D^*)$ base, we have (We should claim that $\tilde{\Phi}_D$ is in the fundamental representation.)

$$\begin{aligned} a_{SU(2)=\square or \bar{\square}}^{J=1/2} &= \frac{\lambda_2^{E^2}}{32\pi} \int_{-1}^{+1} d\cos\theta d^{\frac{1}{2}\frac{1}{2}}_{\frac{1}{2}\frac{1}{2}}(\theta) \begin{pmatrix} \mathcal{T}_s^{+0+0} & 0 \\ 0 & \mathcal{T}_s^{-0^*-0^*} \end{pmatrix} \\ &= \frac{\lambda_2^{E^2}}{32\pi} \int_{-1}^{+1} d\cos\theta \cos\frac{\theta}{2} \begin{pmatrix} -\cos\frac{\theta}{2} & 0 \\ 0 & -\cos\frac{\theta}{2} \end{pmatrix} \\ &= -\frac{\lambda_2^{E^2}}{32\pi}, \end{aligned} \quad (A16)$$

with unitarity bound

$$|\lambda_2^E| < 7.09. \quad (A17)$$

However, an alternative basis $(\bar{L}'_L \tilde{\Phi}_D, L'_L \tilde{\Phi}_D^*)$ gives stronger constraint since the group factor is $+0 + 0$ or $-0^* - 0^*$ $\left\{ \mathcal{F}_{\bar{L}'_L \tilde{\Phi}_D \bar{L}'_L \tilde{\Phi}_D}^{s,1} = \mathcal{F}_{L'_L \tilde{\Phi}_D^* L'_L \tilde{\Phi}_D^*}^{s,1} = N \right.$. In this case, we get

$$\begin{aligned} a_{SU(2)=1}^{J=1/2} &= \frac{\lambda_2^{E^2}}{32\pi} \int_{-1}^{+1} d\cos\theta d^{\frac{1}{2}\frac{1}{2}}_{\frac{1}{2}\frac{1}{2}}(\theta) \begin{pmatrix} N_2 \mathcal{T}_s^{+0+0} & 0 \\ 0 & N_2 \mathcal{T}_s^{-0^*-0^*} \end{pmatrix} \\ &= \frac{\lambda_2^{E^2}}{32\pi} \int_{-1}^{+1} d\cos\theta \cos\frac{\theta}{2} \begin{pmatrix} 2 \times (-\cos\frac{\theta}{2}) & 0 \\ 0 & 2 \times (-\cos\frac{\theta}{2}) \end{pmatrix} \\ &= -\frac{\lambda_2^{E^2}}{16\pi}, \end{aligned} \quad (A18)$$

with the group factor enhancement, the unitarity bound becomes

$$|\lambda_2^E| < 5.01. \quad (A19)$$

-
- [1] G. Aad *et al.* [ATLAS], Phys. Lett. B **716** (2012), 1-29 [[arXiv:1207.7214 \[hep-ex\]](#)].
 - [2] S. Chatrchyan *et al.* [CMS], Phys. Lett. B **716** (2012), 30-61 [[arXiv:1207.7235 \[hep-ex\]](#)].
 - [3] H. Davoudiasl, R. Kitano, T. Li and H. Murayama, Phys. Lett. B **609**, 117-123 (2005) [[arXiv:hep-ph/0405097 \[hep-ph\]](#)].
 - [4] W. Altmannshofer and P. Stangl, Eur. Phys. J. C **81**, no.10, 952 (2021) [[arXiv:2103.13370 \[hep-ph\]](#)].

- [5] J. Aebischer, W. Altmannshofer, D. Guadagnoli, M. Reboud, P. Stangl and D. M. Straub, Eur. Phys. J. C **80** (2020) no.3, 252 [[arXiv:1903.10434 \[hep-ph\]](#)].
- [6] J. Albrecht, S. Reichert and D. van Dyk, Int. J. Mod. Phys. A **33** (2018) no.18n19, 1830016 [[arXiv:1806.05010 \[hep-ex\]](#)].
- [7] Y. Li and C. D. Lü, Sci. Bull. **63** (2018), 267-269 [[arXiv:1808.02990 \[hep-ph\]](#)].
- [8] S. Bifani, S. Descotes-Genon, A. Romero Vidal and M. H. Schune, J. Phys. G **46** (2019) no.2, 023001 [[arXiv:1809.06229 \[hep-ex\]](#)].
- [9] B. Abi *et al.* [Muon g-2], Phys. Rev. Lett. **126**, no.14, 141801 (2021) [[arXiv:2104.03281 \[hep-ex\]](#)].
- [10] L. Di Luzio, M. Kirk, A. Lenz and T. Rauh, JHEP **12**, 009 (2019) [[arXiv:1909.11087 \[hep-ph\]](#)].
- [11] L. Silvestrini and M. Valli, Phys. Lett. B **799**, 135062 (2019) [[arXiv:1812.10913 \[hep-ph\]](#)].
- [12] R. Capdevilla, D. Curtin, Y. Kahn and G. Krnjaic, Phys. Rev. D **103** (2021) no.7, 075028 [[arXiv:2006.16277 \[hep-ph\]](#)].
- [13] D. Buttazzo and P. Paradisi, Phys. Rev. D **104** (2021) no.7, 075021 [[arXiv:2012.02769 \[hep-ph\]](#)].
- [14] R. Capdevilla, D. Curtin, Y. Kahn and G. Krnjaic, Phys. Rev. D **105** (2022) no.1, 015028 [[arXiv:2101.10334 \[hep-ph\]](#)].
- [15] T. Li, J. Pei and W. Zhang, Eur. Phys. J. C **81** (2021) no.7, 671 [[arXiv:2104.03334 \[hep-ph\]](#)].
- [16] W. Ahmed, I. Khan, J. Li, T. Li, S. Raza and W. Zhang, Phys. Lett. B **827** (2022), 136879 [[arXiv:2104.03491 \[hep-ph\]](#)].
- [17] B. Zhu and X. Liu, Sci. China Phys. Mech. Astron. **65** (2022) no.3, 231011 [[arXiv:2104.03238 \[hep-ph\]](#)].
- [18] L. Calibbi, M. L. López-Ibañez, A. Melis and O. Vives, Eur. Phys. J. C **81** (2021) no.10, 929 [[arXiv:2104.03296 \[hep-ph\]](#)].
- [19] G. Arcadi, L. Calibbi, M. Fedele and F. Mescia, Phys. Rev. Lett. **127** (2021) no.6, 061802 [[arXiv:2104.03228 \[hep-ph\]](#)].
- [20] T. Aaltonen *et al.* [CDF], Science **376** (2022) no.6589, 170-176 [[doi:10.1126/science.abk1781](#)].
- [21] C. T. Lu, L. Wu, Y. Wu and B. Zhu, [[arXiv:2204.03796 \[hep-ph\]](#)].
- [22] C. R. Zhu, M. Y. Cui, Z. Q. Xia, Z. H. Yu, X. Huang, Q. Yuan and Y. Z. Fan, [[arXiv:2204.03767 \[astro-ph.HE\]](#)].
- [23] Y. Z. Fan, T. P. Tang, Y. L. S. Tsai and L. Wu, [[arXiv:2204.03693 \[hep-ph\]](#)].

- [24] A. Strumia, [[arXiv:2204.04191 \[hep-ph\]](#)].
- [25] P. Athron, A. Fowlie, C. T. Lu, L. Wu, Y. Wu and B. Zhu, [[arXiv:2204.03996 \[hep-ph\]](#)].
- [26] J. M. Yang and Y. Zhang, [[arXiv:2204.04202 \[hep-ph\]](#)].
- [27] J. de Blas, M. Pierini, L. Reina and L. Silvestrini, [[arXiv:2204.04204 \[hep-ph\]](#)].
- [28] T. P. Tang, M. Abdughani, L. Feng, Y. L. S. Tsai and Y. Z. Fan, [[arXiv:2204.04356 \[hep-ph\]](#)].
- [29] X. K. Du, Z. Li, F. Wang and Y. K. Zhang, [[arXiv:2204.04286 \[hep-ph\]](#)].
- [30] G. Cacciapaglia and F. Sannino, [[arXiv:2204.04514 \[hep-ph\]](#)].
- [31] M. Blennow, P. Coloma, E. Fernández-Martínez and M. González-López, [[arXiv:2204.04559 \[hep-ph\]](#)].
- [32] K. Sakurai, F. Takahashi and W. Yin, [[arXiv:2204.04770 \[hep-ph\]](#)].
- [33] G. W. Yuan, L. Zu, L. Feng, Y. F. Cai and Y. Z. Fan, [[arXiv:2204.04183 \[hep-ph\]](#)].
- [34] B. Y. Zhu, S. Li, J. G. Cheng, R. L. Li and Y. F. Liang, [[arXiv:2204.04688 \[astro-ph.HE\]](#)].
- [35] J. Fan, L. Li, T. Liu and K. F. Lyu, [[arXiv:2204.04805 \[hep-ph\]](#)].
- [36] X. Liu, S. Y. Guo, B. Zhu and Y. Li, [[arXiv:2204.04834 \[hep-ph\]](#)].
- [37] H. M. Lee and K. Yamashita, [[arXiv:2204.05024 \[hep-ph\]](#)].
- [38] Y. Cheng, X. G. He, Z. L. Huang and M. W. Li, [[arXiv:2204.05031 \[hep-ph\]](#)].
- [39] H. Song, W. Su and M. Zhang, [[arXiv:2204.05085 \[hep-ph\]](#)].
- [40] E. Bagnaschi, J. Ellis, M. Madigan, K. Mimasu, V. Sanz and T. You, [[arXiv:2204.05260 \[hep-ph\]](#)].
- [41] A. Paul and M. Valli, [[arXiv:2204.05267 \[hep-ph\]](#)].
- [42] H. Bahl, J. Braathen and G. Weiglein, [[arXiv:2204.05269 \[hep-ph\]](#)].
- [43] P. Asadi, C. Cesarotti, K. Fraser, S. Homiller and A. Parikh, [[arXiv:2204.05283 \[hep-ph\]](#)].
- [44] L. Di Luzio, R. Gröber and P. Paradisi, [[arXiv:2204.05284 \[hep-ph\]](#)].
- [45] P. Athron, M. Bach, D. H. J. Jacob, W. Kotlarski, D. Stöckinger and A. Voigt, [[arXiv:2204.05285 \[hep-ph\]](#)].
- [46] J. Gu, Z. Liu, T. Ma and J. Shu, [[arXiv:2204.05296 \[hep-ph\]](#)].
- [47] K. S. Babu, S. Jana and V. P. K., [[arXiv:2204.05303 \[hep-ph\]](#)].
- [48] J. J. Heckman, [[arXiv:2204.05302 \[hep-ph\]](#)].
- [49] Y. H. Ahn, S. K. Kang and R. Ramos, [[arXiv:2204.06485 \[hep-ph\]](#)].
- [50] X. F. Han, F. Wang, L. Wang, J. M. Yang and Y. Zhang, [[arXiv:2204.06505 \[hep-ph\]](#)].
- [51] M. D. Zheng, F. Z. Chen and H. H. Zhang, [[arXiv:2204.06541 \[hep-ph\]](#)].

- [52] K. I. Nagao, T. Nomura and H. Okada, [[arXiv:2204.07411 \[hep-ph\]](#)].
- [53] T. A. Chowdhury, J. Heeck, S. Saad and A. Thapa, [[arXiv:2204.08390 \[hep-ph\]](#)].
- [54] G. Arcadi and A. Djouadi, [[arXiv:2204.08406 \[hep-ph\]](#)].
- [55] K. Ghorbani and P. Ghorbani, [[arXiv:2204.09001 \[hep-ph\]](#)].
- [56] S. Lee, K. Cheung, J. Kim, C. T. Lu and J. Song, [[arXiv:2204.10338 \[hep-ph\]](#)].
- [57] R. Benbrik, M. Boukidi and B. Manaut, [[arXiv:2204.11755 \[hep-ph\]](#)].
- [58] H. Abouabid, A. Arhrib, R. Benbrik, M. Krab and M. Ouchemhou, [[arXiv:2204.12018 \[hep-ph\]](#)].
- [59] Y. Heo, D. W. Jung and J. S. Lee, [[arXiv:2204.05728 \[hep-ph\]](#)].
- [60] T. Biekötter, S. Heinemeyer and G. Weiglein, [[arXiv:2204.05975 \[hep-ph\]](#)].
- [61] L. Calibbi, T. Li, Y. Li and B. Zhu, JHEP **10**, 070 (2020) [[arXiv:1912.02676 \[hep-ph\]](#)].
- [62] M. Sabir, W. Ahmed, Y. Gong, T. Li and J. Lin, JCAP **09**, 038 (2020) [[arXiv:1908.05201 \[hep-ph\]](#)].
- [63] E. Aprile *et al.* [XENON], Phys. Rev. D **102**, no.7, 072004 (2020) [[arXiv:2006.09721 \[hep-ex\]](#)].
- [64] L. Allwicher, P. Arnan, D. Barducci and M. Nardecchia, JHEP **10**, 129 (2021) [[arXiv:2108.00013 \[hep-ph\]](#)].
- [65] M. E. Peskin and T. Takeuchi, Phys. Rev. Lett. **65** (1990), 964-967 [[doi:10.1103/PhysRevLett.65.964](#)]
- [66] M. E. Peskin and T. Takeuchi, Phys. Rev. D **46** (1992), 381-409 [[doi:10.1103/PhysRevD.46.381](#)]